

Enhancement of Field Oriented Control for Permanent Magnetic Synchronous Motor using Ant Colony Optimization

MERIE MEGRINI, AHMED GAGA, YOUNESS MEHDAOUI

Research Laboratory of Physics and Engineers Sciences (LRPSI),

Research Team in Embedded Systems, Engineering, Automation, Signal, Telecommunications and Intelligent Materials (ISASTM),

Polydisciplinary Faculty (FPBM), Sultan Moulay,

Slimane University (USMS),

Beni Mellal,

MOROCCO

Abstract: - Because of its frequent use in diverse systems, the PMSM drive must be controlled. Field-oriented control (FOC) based PMSM drive is modeled in the present work to optimize the torque and speed performance of the PMSM. The FOC is based on a dissociated speed and flux control approach, which controls the speed and flux of the PMSM independently. The standard Proportional Integrator Derivative (PID) controller regulates the speed in FOC, which is noted for its increased resilience in linear systems, however in nonlinear ones, the PID controller responds poorly to changes in the system's variables. In this case, the best solutions are frequently based on optimization techniques that produce the controller's gains in every period. Optimizing the PID's behavior in response to the system's nonlinear behavior. The novel proposed strategy for enhancing the gains of the PID controller by employing a cost function such as Integral Time Absolute Error (ITAE) is based on PID speed regulation and is optimized using the Ant Colony Optimization algorithm (ACO) for FOC. To confirm the strategy's aims, the suggested method is implemented on Matlab/Simulink. The simulation results demonstrated the efficiency of the intelligent ACO-FOC control, which delivers good performance in terms of stability, rapidity, and torque fluctuations.

Key-Words: - Ant colony optimization, Field oriented control, Permanent magnetic synchronous motor, Proportional integral derivative, Park transformation, Park inverse transformation.

Received: February 16, 2023. Revised: December 2, 2023. Accepted: December 14, 2023. Published: March 1, 2024.

1 Introduction

Researchers have already been grappling with the regulation of variable-speed electrical machinery since the birth of industrialization. This is why electrical motors are becoming increasingly demanding in terms of efficiency, dependability, and cost reduction, [1], [2], [3]. This difficulty was rectified in the nineteenth century with DC motors; however, these drives cannot be utilized in corrosive environments or high-power levels and the commutator also requires repair, [4], [5]. As a result of these limits, research on the subject of variable speed has been oriented toward AC machines, particularly synchronous machines.

Permanent Magnet Synchronous Motors (PMSM) provide several advantages, including a high-power factor, a high-power density, high efficiency, and low-maintenance operation, [6], [7].

Multiple methods are utilized in the field of controls, which have advantages but are limited by

some drawbacks; among these popular controls that have been used on PMSM is the Field Oriented Control (FOC), whose operating principle is to restore the function of the PMSM to that of a DC machine, ensuring an uncoupling of flux and torque, [8], [9]. However, in the case of Sensored or Direct Field Oriented Control (DFOC), [9], this technique needs a sensor located in the air gap to precisely determine the flux, and the sensors are susceptible to physical and mechanical restrictions (temperature, vibration), [10]. Sensorless or indirect Field Oriented Control (IFOC) eliminates the flux sensor problem but has the disadvantage of being sensitive to machine parameter fluctuations, particularly the rotor and stator time constant. Furthermore, this technique necessitates the use of six traditional PID regulators, making the control complex and sensitive to parameter variations, [11]. For this reason DFOC how will used in this work. By far the most often utilized controller in virtually all industrial control applications is the proportional-

integral-derivative (PID) controller. Over ninety percent of all control loops are PID, spanning applications ranging from process management to motor drives, transportation, and aviation control. Because of their linear form, these linear control techniques have the benefit of being simple to implement and simple to synthesize. Its applications will be unsuccessful, especially if the structures that have to be controlled have complex and nonlinear properties, [12], and because of the PID regulator's renowned characteristics, which fail to be adaptable when the system is nonlinear and complex, and because its gains rely on machine settings that are variable due to physical constraints, [13]. As a result, various research efforts have been made to address the shortcomings of the PID controller in changeable parameter systems. For optimum performance of the PID controller, intelligent optimization techniques such as Particle Swarm Optimization (PSO) [14], autotuning [15], Fuzzy Logic [16], Genetic Algorithm (GA) [17], [18], [19], Evolutionary Programming (EP) [20] and Future Search Algorithm (FSA) [21], have been used.

A PID regulator tuned using an ACO technique is employed in this study to control the speed of the PMSM using DFOC. ACO has attracted widespread interest and use in addressing continuous non-linear optimization problems due to its ease of implementation, simple principle, and rapid convergence.

Ant colony Optimization is a strategy for optimization inspired by the feeding behavior of genuine ant colonies. It was originally suggested in 1992 by Marco Dorigo. ACO is used in [22], for Dynamic path optimization; it is a crucial part of intelligent transportation systems. Where the results are more accurate. The application of Ant Colony Optimization in [23], is in the field of Image Processing. Application/Improvements: ACO has been used successfully in a variety of applications that deal with images such as edge linking, edge detection, segmentation, image compression, and feature extraction. ACO is also widely used to modify and improve the gains of PID controllers. T. Sakthivel and Co. ACO was introduced in [24], [25] to identify optimal PID regulator gains for the Doubly Field Induction Motor (DFIM) and Induction Motor (IM), respectively. For a variety of reasons, including the ability to reply at a faster rate and with no static error in response speed, employing ACO to control the speed of the PMSM using DFOC is useful. The work in this paper focuses on the analytical analysis and design of FOC control applied to PMSM, and the parameters

of the PID speed controller are optimized utilizing the ACO algorithm by ITAE cost functions. This study will be analyzed using a Matlab/Simulink environment. Figure 1 depicts the overall framework of the proposed control system.

The following sections comprise this article: The second section is devoted to the development of the FOC strategy and the PMSM mathematical model. Section 3 is concerned with the development and design of the ACO algorithm. Section 4 is dedicated to the implementation of the ACO-FOC intelligent strategy on Matlab/Simulink, as well as the discussion of simulation results. Section 5 is for concluding the work.

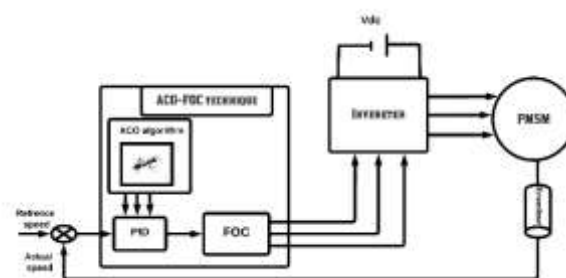


Fig. 1: ACO-FOC control structure

2 Overview of FOC for PMSM Drive

2.1 FOC Strategy

First, FOC is an algorithm that controls the PMSM motor as if it were a DC motor. Whereas the mathematical model of PMSM generates nonlinear equations and has torque and flux equations dependent on each other, making PMSM management problematic. However, as a result of the FOC method, the torque and flux equations become independent. As a result, the control will be simpler than the first.

The FOC algorithm is built around two essential concepts: The first fundamental principle is that of flux and torque producing currents, [26], and the second is that of reference frames. A reference frame is used to convert a sinusoidal quantity in one reference frame to a constant value in another reference frame that rotates at the same frequency. As a result, FOC control is accomplished through these procedures; After measuring the three phase currents I_a , I_b , and I_c , the park transformation is used to transition from a sinusoidal current and a stationary frame to a constant current (I_q , I_d) and a rotating frame. The Park transformation converts a sinusoidal quantity in a stationary reference frame from a three-phase reference to a two-phase reference. The matrix below is utilized to do this transformation.

$$P(\theta_s) = \sqrt{\frac{2}{3}} \begin{pmatrix} \cos(\theta) & \cos(\theta - \frac{2\pi}{3}) & \cos(\theta - \frac{4\pi}{3}) \\ -\sin(\theta) & -\sin(\theta - \frac{2\pi}{3}) & -\sin(\theta - \frac{4\pi}{3}) \\ \frac{1}{\sqrt{2}} & \frac{1}{\sqrt{2}} & \frac{1}{\sqrt{2}} \end{pmatrix} \quad (1)$$

Park inverse transformation is from the dq frame into a, b, and c frames. To do it, the matrix below is used.

$$P(\theta_s)^{-1} = \sqrt{\frac{2}{3}} \begin{pmatrix} \cos(\theta) & -\sin(\theta) & \frac{1}{\sqrt{2}} \\ \cos(\theta - \frac{2\pi}{3}) & -\sin(\theta - \frac{2\pi}{3}) & \frac{1}{\sqrt{2}} \\ \cos(\theta - \frac{4\pi}{3}) & -\sin(\theta - \frac{4\pi}{3}) & \frac{1}{\sqrt{2}} \end{pmatrix} \quad (2)$$

2.2 Modelling of PMSM drive

A Permanent Magnet Synchronous Motor (PMSM) is an electric motor that generates a magnetic field using permanent magnets integrated into the rotor. It is a synchronous motor, which implies that the rotor's rotational speed is synchronized with the frequency of the applied electrical current. PMSM motors are commonly built to run on three-phase alternating current (AC). To generate a rotating magnetic field, the stator windings are typically organized in three stages, each displaced by 120 degrees (Figure 2), Table 2 (Appendix) shows the PMSM motor parameters used in this work.

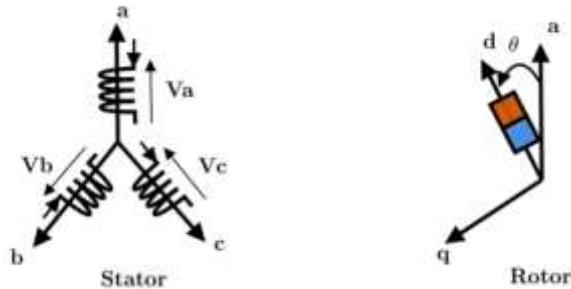


Fig. 2: PMSM representation's stator and rotor

The dynamic model of the PMSM is determined utilizing the 2-phase motor direct and quadrature axes. The PMSM dq-model is generated from the synchronous machine's winding and field current dynamics. The PMSM dynamic model is developed using only a few assumptions. Stator winding has an identical amount of turns when the three-phase supply voltage is balanced. The induced EMF has sinusoidal characteristics, and hysteresis losses, ripples, and saturation are not taken into account. The PARK transformation notion simplifies the derivation of electrical equations even further. The mathematical representation of the PMSM motor will be written as follows and Table 1 (Appendix) presents the list of the symbols used:

- The equations in the three-phase frame are as follows:

-The stator's voltage is expressed as:

$$\begin{cases} [V_a] = [R][I_a] + \frac{d[\phi_a]}{dt} \\ [V_b] = [R][I_b] + \frac{d[\phi_b]}{dt} \\ [V_c] = [R][I_c] + \frac{d[\phi_c]}{dt} \end{cases} \quad (3)$$

-The stator's flux expressed as:

$$\begin{cases} [\phi_a] = [L_s][I_a] + [M][I_f] \\ [\phi_b] = [L_s][I_b] + [M][I_f] \\ [\phi_c] = [L_s][I_c] + [M][I_f] \end{cases} \quad (4)$$

-The dynamic equation is as follows:

$$J \frac{d\Omega}{dt} = T_{em} - T_r - T_f \quad (5)$$

- The stator equation on the dq coordinate can be given as:

-The stator's voltage is as follows:

$$\begin{bmatrix} V_{ds} \\ V_{qs} \end{bmatrix} = P(\theta_s) \cdot \begin{bmatrix} V_a \\ V_b \\ V_c \end{bmatrix} \quad (6)$$

$$\begin{cases} V_{ds} = R_s \cdot i_{ds} + \frac{d\phi_{ds}}{dt} - \omega_r \phi_{qs} \\ V_{qs} = R_s \cdot i_{qs} + \frac{d\phi_{qs}}{dt} + \omega_r \phi_{ds} \end{cases} \quad (7)$$

-The stator's flux expressed as:

$$\begin{bmatrix} \phi_{ds} \\ \phi_{qs} \end{bmatrix} = P(\theta_s) \cdot \begin{bmatrix} \phi_a \\ \phi_b \\ \phi_c \end{bmatrix} \quad (8)$$

$$\begin{cases} \phi_{ds} = L_{ds} \cdot i_{ds} + M \cdot i_{dr} \\ \phi_{qs} = L_{qs} \cdot i_{qs} + M \cdot i_{qr} \end{cases} \quad (9)$$

-The electromagnetic torque generated by the PMSM is presented below as a function of stator quadrature current and flux.

$$T_{em} = p \cdot [\phi_{ds} \cdot i_{qs} - \phi_{qs} \cdot i_{ds}] \quad (10)$$

-The electromagnetic torque is simplified using the stator field-oriented control strategy ($i_d = 0$) and becomes as follows:

$$T_{em} = p \cdot \phi_{ds} \cdot i_{qs} \quad (11)$$

3 ACO Controlling Mechanism for PMSM Drive Solution

The ACO method based on how ants behave while looking for food. The ants start by moving randomly. After seeking food, they back to the colony, signaling their path using pheromones, [27]. When more ants encounter this path, they are more inclined to halt their chaotic motions and follow the

prescribed path, so strengthening the trail on their way back if the designated road leads to food. Simultaneously, the shorter way will be used with greater frequency, strengthening and tempting it, [24]. A network scenario can be used to depict the challenge of developing the PID controller utilizing the ACO algorithm (Figure 3). Three separate vectors were used to organize all of the information for each gain (P, I, D). The vectors in question can be thought of as roads connecting nests to form a graphical representation of the scenario. During the journey, each ant must navigate three colonies by selecting the best route between the start and end nodes. The purpose of the ACO is to discover the best route with the lowest cost function around the three colonies. These ants deposit their pheromones at the beginning of each trail.

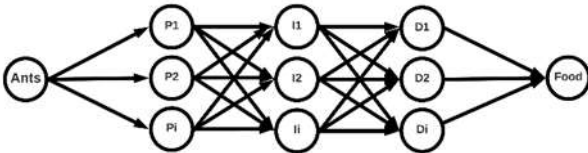


Fig. 3: ACO structure as a neural network problem

Important steps in the implementation of the ACO include choosing the cost functions that will be used to assess each node's appropriateness. The three cost functions used frequently are integral square error (ISE), integral absolute error (IAE), and integral time absolute error (ITAE). Where the ITAE will be employed for this work. Equation 12 expresses it.

$$ITAE(e) = \sum_{i=1}^n i|e_i| \quad (12)$$

The optimization of the PID controller utilizing the ACO block structure is shown in Figure 4.

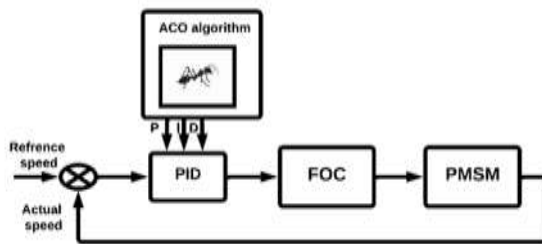


Fig. 4: PID Controller Optimization Using ACO

Figure 5 depicts the sequence of operations required to build the given ACO algorithm and Table 3 (Appendix) shows The ACO parameters utilized in the current study.



Fig. 5: ACO Sequence for PID Controller optimization

4 Simulation and Discussion

The proposed speed and torque control using the FOC-ACO block scheme is shown in Figure 6, where, the inverter with the machine and the control, is built on SIMULINK and the algorithmic part is done on Matlab. That is, the gains values of the ACO-optimized speed PID regulator are all produced using MATLAB, and the control takes place in SIMULINK. Where the PMSM is configured using the parameters listed in Table 2 (Appendix).

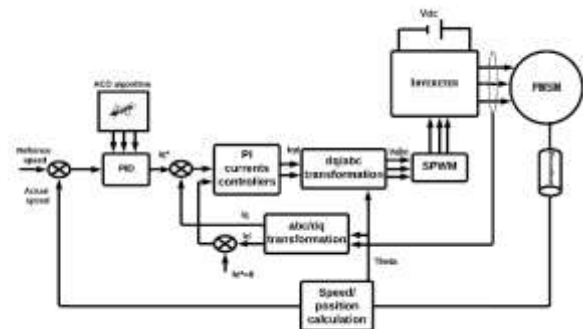


Fig. 6: ACO-FOC control structure of the PMSM

During simulation, two scenarios are studied for the examination of field-oriented control: variable load with variable reference speed and dynamic speed with no load. The simulation results are depicted in the following figures.

4.1 Under No Load

As shown in Figure 7-a, the PMSM is in acceleration mode. Where there is no load, the speed increased from 80 rad/s to 110 rad/s at $t=3$ s. The torque response of the system is shown in Figure 7-b, and the load torque follows the electromagnetic torque, which has a value of 0 Nm. The quadrature current generated by the ACO method speed regulation is represented in Figure 7-c which is equal to zero. Figure 7-d shows the direct current, which is 0 due to the proximity of FOC.

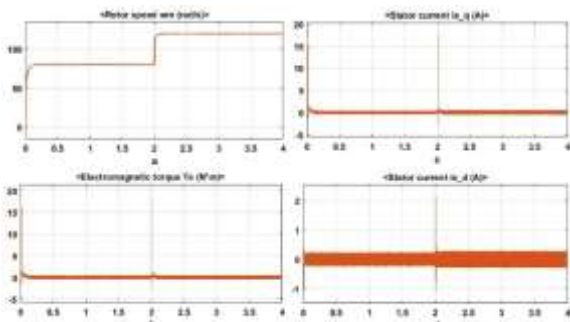


Fig. 7: Response under no load: a- Speed response, b- Torque response, c- Quadrature current, d- Direct current

The settling time is 0.06 s with no overshoot and no peak time of the speed as shown in Figure 8-a. The torque, as seen in Figure 8-b, follows the quadrature current path (Figure 8-c), thanks to the ACO-FOC method, which allows for torque control by adjusting the proportionate quadrature currents and as presented in their responses there is small ripple that render this control well performed. Figure 8-d shows that the flux has been oriented, causing the direct current to equal zero.

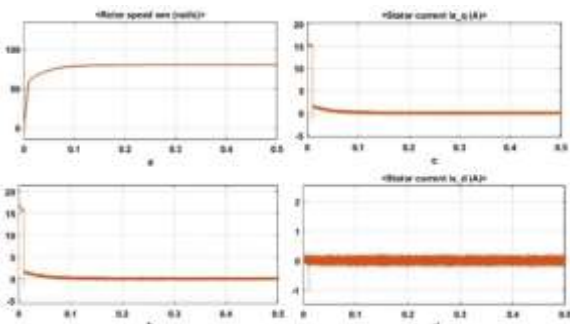


Fig. 8: Zoom response under load: a- Speed response, b- Torque response, c- Quadrature current, d- Direct current

4.2 Under Load

PMSM is in acceleration mode, as seen in Figure 9-a. At $t=3$ s, the speed rose from 80 rad/s to 110 rad/s under a variable load. The system's torque response is depicted in Figure 9-b, and the load torque follows the electromagnetic torque, which has 10Nm in the first 3s and -10Nm after that. The quadrature current generated from the speed regulation using the ACO algorithm is depicted in Figure 9-c. Figure 9-d depicts the direct current, which is equal to zero.

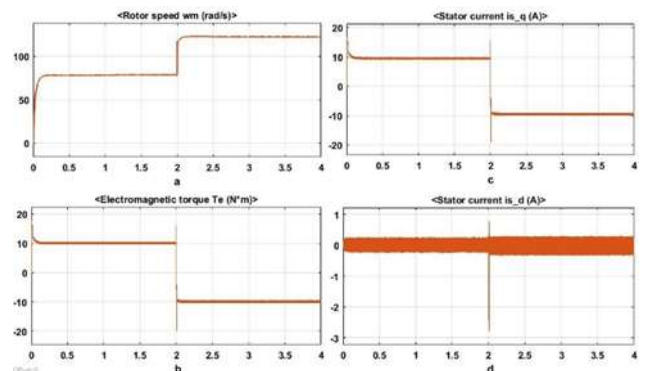


Fig. 9: Response under load: a- Speed response, b- Torque response, c- Quadrature current, d- Direct current

The settling time is 0.15 s with no overshoot and no peak time of the speed is shown in Figure 10-a. The torque, as seen in Figure 10-b, follows the quadrature current path (Figure 10-c), thanks to the FOC method, which allows for torque control by adjusting the proportionate quadrature currents. Figure 10-d shows that the flux has been oriented, causing the direct current to equal zero.

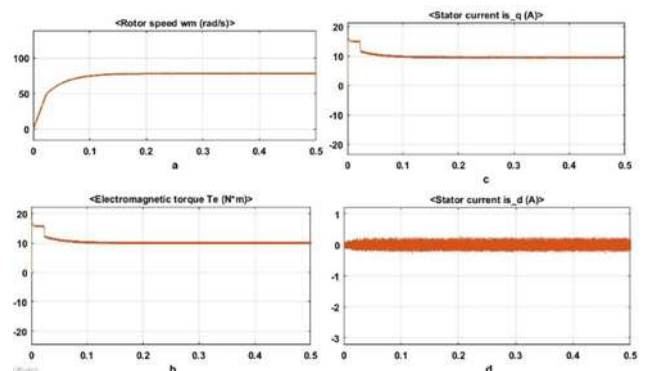


Fig. 10: Zoom response under load: a- Speed response, b- Torque response, c- Quadrature current, d- Direct current

Figure 11-a displays the acceleration and deceleration speed performance of the PMSM using the ACO-FOC algorithm to optimize the PID gains, which results in good performance (Figure 11-a), as well as the reliability of ACO-FOC in torque control utilizing current control (Figure 11-b). Where the motor accelerates to 100 rad/s, and decelerates to -100 rad/s after 3 seconds (Figure 11-a) with the same performance discussed previously. Furthermore, Figure 11-b depicts the performance of the ACO-FOC control under varying loads, implying that a variable quadrature current (Figure 11-c) follows the same electromagnetic torque path. As illustrated in the Figure 11-b and Figure 11-c, there are little ripples and good control of current and torque. Furthermore, Figure 11-d shows that this control is reliable where the quadrature current is still zero.

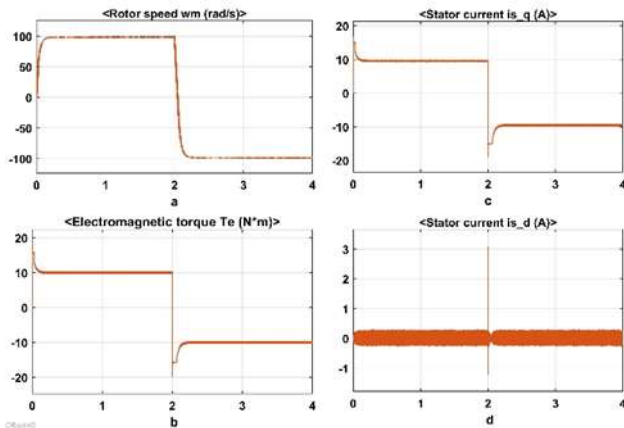


Fig. 11: Response under load: a- Acceleration and deceleration of speed response, b- Torque response, c- Quadrature current, d- Direct current

5 Conclusion

In this paper, an optimization technique known in terms of ACO implemented in PMSM using the FOC strategy is used to optimize the PID gains that are used to regulate the PMSM speed. The simulation results of ACO-PID for speed control confirm that this algorithm is well performed due to the response that has less settling time, no overshoot, no peak time, and reduced the steady state error.

What's more the response of torque has fewer ripples owing to the FOC strategy. In addition, due to this strategy, both currents; quadrature and direct are well regulated.

Though successful in the Matlab/Simulink environment, the proposed FOC approach and ACO algorithm have not yet been put into practice in real

time using embedded systems and PMSM motors. Numerous applications, such as robotics and ventilation, but particularly electric automobiles, call for the usage of this system.

References:

- [1] N. El Ouanjli, A. Derouich, el ghizal Abdelaziz, C. Ali, M. Taoussi, et B. Bossoufi, Direct Torque Control Strategy Based on Fuzzy Logic Controller for a Doubly Fed Induction Motor, *IOP Conference Series: Earth and Environmental Science*, vol. 161, p. 012004, 2018, doi: 10.1088/1755-1315/161/1/012004.
- [2] M. Mossa, D. Echeikh, et A. Iqbal, Enhanced control technique for a sensor-less wind driven doubly fed induction generator for energy conversion purpose, *Energy Reports*, vol. 7, p. 5815-5833, 2021, doi: 10.1016/j.egy.2021.08.183.
- [3] M. Mossa, T. Do, A. Al-Sumaiti, et A. Diab, Cost-Effective Predictive Flux Control for a Sensorless Doubly Fed Induction Generator, *IEEE Access*, vol. PP, p. 1-1, 2019, doi: 10.1109/ACCESS.2019.2951361.
- [4] B. Adhavan, A. Kuppaswamy, G. Jayabaskaran, et V. Jagannathan, Field oriented control of Permanent Magnet Synchronous Motor (PMSM) using fuzzy logic controller, *IEEE Recent Advances in Intelligent Computational Systems*, in 2011, Trivandrum, India: IEEE, 2011, p. 587-592. doi: 10.1109/RAICS.2011.6069379.
- [5] M. Mossa, S. Bolognani, Effective model predictive direct torque control for an induction motor drive. 2016, p. 754, 2016 *International Symposium on Power Electronics, Electrical Drives, Automation and Motion (SPEEDAM)*, doi: 10.1109/SPEEDAM.2016.7525814.
- [6] S. Muthurajan, R. Loganathan, et R. R. Hemamalini, Deep Reinforcement Learning Algorithm based PMSM Motor Control for Energy Management of Hybrid Electric Vehicles, *WSEAS Transactions on Power Systems*, vol. 18, p.18-25, 2023, <https://doi.org/10.37394/232016.2023.18.3>
- [7] S. Drid, M.-S. Nait-said, et M. Tadjine, Double Flux Oriented Control for the Doubly Fed Induction Motor, *Electric Power Components and Systems*, vol. 33, p. 2005, oct. 2005, doi: 10.1080/15325000590933483.
- [8] M. Said, A. Derouich, N. El Ouanjli, E. M. Mohammed, et M. Taoussi, A New Strategy-

- Based PID Controller Optimized by Genetic Algorithm for DTC of the Doubly Fed Induction Motor, *Systems*, vol. 9, p. 37, 2021, doi: 10.3390/systems9020037.
- [9] L. Amezquita-Brooks, E. Liceaga-Castro, J. Liceaga, et C. Ugalde-Loo, Flux-torque cross-coupling analysis of FOC schemes: Novel perturbation rejection characteristics, *ISA transactions*, vol. 59, 2015, doi: 10.1016/j.isatra.2015.05.004.
- [10] M. Mossa, D. Echeikh, et N. Quynh, A Novel Sensorless Predictive Voltage Control for an Induction Motor Drive Based on a Back-Stepping Observer-Experimental Validation, *IEEE Access*, vol. 9, 2021, doi: 10.1109/ACCESS.2021.3051436.
- [11] A. Jayachitra et V. Rajendran, Genetic Algorithm Based PID Controller Tuning Approach for Continuous Stirred Tank Reactor, *Advances in Artificial Intelligence*, vol. 2014, p.1-8, 2014, doi: 10.1155/2014/791230.
- [12] H. Feng, C. Yin, W. Weng, W. Ma, J. Zhou, W. Jia, Z. Zhang, Robotic excavator trajectory control using an improved GA based PID controller, *Mechanical Systems and Signal Processing*, vol. 105, p. 153-168, 2018, doi: 10.1016/j.ymsp.2017.12.014.
- [13] Y. Ye, C.-B. Yin, Y. Gong, J. Zhou, Position control of nonlinear hydraulic system using an improved PSO based PID controller, *Mechanical Systems and Signal Processing*, vol. 83, p. 241-259, 2017, doi: 10.1016/j.ymsp.2016.06.010.
- [14] M. M. Abdo, A. R. Vali, A. R. Toloei, M. R. Arvan, Stabilization loop of a two axes gimbal system using self-tuning PID type fuzzy controller, *ISA Transactions*, vol. 53, no 2, p. 591-602, 2014, doi: 10.1016/j.isatra.2013.12.008.
- [15] M. Said, A. Derouich, A. Iqbal, et N. El Ouanjli, ANT colony optimization direct torque control for a doubly fed induction motor, *Energy Reports*, vol. 8, p.81-98, 2022, doi: 10.1016/j.egyr.2021.11.239.
- [16] M. Elsis, M. Soliman, M. Aboeela, et W. Mansour, GSA-Based Design of Dual Proportional Integral Load Frequency Controllers for Nonlinear Hydrothermal Power System, *World Academy of Science, Engineering and Technology*, vol. 9, p. 1142-1148, 2015.
- [17] Y. Wang, Q. Jin, R. Zhang, improved fuzzy PID controller design using predictive functional control structure, *ISA Transactions*, vol. 71, p. 354-363, 2017, doi: 10.1016/j.isatra.2017.09.005.
- [18] Y.-Y. Hou, Design and implementation of EP-based PID controller for chaos synchronization of Rikitake circuit systems, *ISA Transactions*, vol. 70, p. 260-268, 2017, doi: 10.1016/j.isatra.2017.04.016.
- [19] M. Elsis et M. Soliman, Optimal design of robust resilient automatic voltage regulators, *ISA Transactions*, vol. 108, p. 257-268, 2021, doi: 10.1016/j.isatra.2020.09.003.
- [20] J. Cheng, Dynamic Path Optimization Based on Improved Ant Colony Algorithm, *Journal of Advanced Transportation*, vol. 2023, p. 1-11, 2023, doi: 10.1155/2023/7651100.
- [21] N. Siddiqui, D.-S. Abbas, Image Processing Using Ant Colony Optimization, *JETIR*, vol. 6, p. 946-953, 2019.
- [22] M. Said, A. Derouich, N. El Ouanjli, N. Quynh, M. Mossa, A New Hybrid Ant Colony Optimization Based PID of the Direct Torque Control for a Doubly Fed Induction Motor, *World Electr. Veh. J.* 2022, vol. 13, 2022. doi: 10.3390/wevj13050078.
- [23] Y. Dhieb, M. Yaich, A. Guermazi, et M. Ghariani, PID Controller Tuning using Ant Colony Optimization for Induction Motor, *Journal of Electrical Systems*, vol. 15, p. 133-141, 2019.
- [24] R.B.Gimenez, *High Performance Sensorless Vector Control of Induction Motor Drive*, University of Nottingham, December, 1995.
- [25] M. Dorigo, M. Birattari, et T. Stutzle, Ant colony optimization *IEEE Comput. Intell. Mag.*, vol. 1, no 4, p. 28-39, 2006, doi:10.1109/MCI.2006.329691.
- [26] H. B. Achour, S. Ziani, Y. Chaou, Y. El Hassouani, A. Daoudia, Permanent Magnet Synchronous Motor PMSM Control by Combining Vector and PI Controller, *WSEAS Transactions on Systems and Control*, vol. 17, p. 244-249, 2022, <https://doi.org/10.37394/23203.2022.17.28>.
- [27] M. Dorigo, M. Birattari, et T. Stutzle, Ant colony optimization *IEEE Comput. Intell. Mag.*, vol. 1, no 4, p. 28-39, 2006, doi:10.1109/MCI.2006.329691

APPENDIX

Table 1. List of symbols

Parameters	Description
V_a, V_b, V_c	Stator three phases voltage
R	Stator resistance
L_s	Stator inductance
ϕ_{ds}, ϕ_{qs}	Quadrature and direct flux
ω_r, θ	Rotor angular Speed, position
M	Mutual inductance
J	Inertia
V_{ds}, V_{qs}	Stator two phases voltage
T_s, T_{em}, T_r, T_f	Electromagnetic torque, Resistant torque, Viscous friction coefficient
P, I, D	PID gains
V_{dc}	DC voltage
e	Speed error

Table 2. PMSM motor parameters

Parameters	Value
Flux linkage	0.175
R	0.2
L_s	8.5 e-3
P	4
J	0.0027
T_f	0
VDC	400

Table 3. ACO parameters

Parameters	Value
n_iter	5
NA	30
Evaporation	0.7
Alpha	1
beta	0.85
n_node	1000
n_param	3

Contribution of Individual Authors to the Creation of a Scientific Article (Ghostwriting Policy)

Miss. MEGRINI Meriem: Methodology, Funding acquisition, formal analysis, writing.

Mr. GAGA Ahmed: Methodology, supervision, validation.

Mr. MEHDOUI Youness: supervision, validation.

Sources of Funding for Research Presented in a Scientific Article or Scientific Article Itself

No funding was received for conducting this study.

Conflict of Interest

The authors have no conflicts of interest to declare.

Creative Commons Attribution License 4.0 (Attribution 4.0 International, CC BY 4.0)

This article is published under the terms of the Creative Commons Attribution License 4.0

https://creativecommons.org/licenses/by/4.0/deed.en_US